Low-Activation Reinforced Concrete Design Methodology (11) -Preliminary FEM Analysis of Thermal Stress for Low-Activation Concrete -

Yusuke Fujikura[1)], Hirokazu Nishida[1)], Norichika Katayose[1)], Ken-ichi Kimura[1)], Masaharu Kinno[1)], and Akira Hasegawa[2)]

1) Technology Development Division, Fujita Corporation, Atsugi, Japan
2) Tohoku University, Sendai, Japan

ABSTRACT

In order to reduce long-lived residual radionuclide in a concrete shielding around a reactor, we newly developed two types of low-activation concrete, namely, "1/10-low-activation concrete" and "1/30-low-activation concrete". The physical and mechanical properties of these concrete were tested by the experimental works. The thermal stress generated by cement hydration was calculated by the three dimension FEM analysis targeting massive concrete in the reactor. Upon this study, we evaluated the realization of two types of low-activation concrete, and assessed the utilization for applying the above low-activation concrete to the reactor shielding wall, by comparing the experimental data to the calculated data. The evaluation conducted the 1/10-low-activation concrete was effective for the use of the shielding wall.

INTRODUCTION

Concrete is very practical and inexpensive material for radiation shielding. While, after a long period of operation, the shielding concrete around a nuclear reactor change to low level radioactive waste because of the remaining long lived radionuclides. The disposal cost of this activated concrete is considered to be a hundred times expensive compared to that of non-activated concrete. This calls for the reduction of radioactive concrete to "clearance level" from a viewpoint of cost savings and reutilization of natural resources. Here, "clearance level" denotes the radioactive classification permissible for disposing of material as non-radioactive waste.

In order to reduce the residual radionuclides in a concrete shield around a reactor, we developed several types of low-activation concrete [1]. Generally, a reactor shielding wall consists of a large section of member, and of massive concrete. The evaluation of crack generation in massive concrete due to cement hydration is, therefore, indispensable. However, no systematic study on crack generation of low-activation concrete regarding the shielding wall have been studied up to this time.

The objective of this work is to establish an evaluation system of mix proportion design regarding avoiding crack generation of low-activation concrete by the experimental data and the FEM (finite element method) thermal stress calculation system.

PROPERTIES OF LOW-ACTIVATION CONCRETE

Low-activation materials and mix proportions of concrete

Screening tests using the thermal reactor JRR-4 of the Japan Atomic Energy Agency were performed to identify low-activation raw materials for concrete that can be used for nuclear facilities. About 300 specimens of aggregate and cement were chosen. The dominant long-lived residual radionuclides induced in concrete are, in order of importance, ^{152}Eu (representative single value of the clearance level of IAEA-RS-G1.7 [2], C_{152Eu} = 0.1 Bq/g, half-life ($T_{1/2}$) = 13.54 yr), ^{60}Co (C_{60Co} = 0.1 Bq/g, $T_{1/2}$ = 5.271 yr), and ^{154}Eu (C_{154Eu} = 0.1 Bq/g, $T_{1/2}$ = 8.593 yr), produced by ^{151}Eu (n, γ), ^{60}Co (n, γ), and ^{153}Eu (n, γ) reactions, respectively. These radionuclides are known to occupy 99-100 % of the total residual radioactivity induced in ordinary concrete at the time of decommissioning[3]. The dominant target elements of concrete shield is, therefore, Eu and Co. Table 1 presents the dominant target elements of reference materials obtained by such screening tests.

Here, we composed two types of concrete as shown in Table 2, namely, "1/10-low-activation concrete" and "1/30-low-activation concrete". The reduction rate of the activation for the 1/10-low-activation concrete is designed to be 1/10 compared to the andesite concrete which is considered to be "ordinary concrete". That for the 1/30-low-activation concrete is designed to be 1/30. The densities and the water absorption rates are presented in Table 3. The compressive strength, slump, and air content are designed as 33N/mm^2, 15±2.5cm, and 4±1%, respectively.

Test and inspection

The items of the test and the criteria used in this study are listed in Table 4. We measured the properties of fresh concrete, mechanical properties of the hardened concrete and the adiabatic temperature rise as the cement hydration. Here, "JIS", "JASS", and "JCI" denote "Japanese Industrial Standard", "Japanese Architectural Standard Specification", and "Japanese Concrete Institute", respectively. The bleeding water related to the physical properties

of the hardened concrete was also measured according to JIS A 1123. The setting time for each execution was automatically measured according to JIS A 1147. The compressive and the splitting tensile strength of the executed concrete were measured using the cylindrical test specimen of 100 mm in diameter and 200 mm in height. The test specimens were cured in water at 20 ºC, for the periods of 7 days, 28 days, and 91 days. The adiabatic temperature rise related to the crack generation in massive concrete was measured according to JCI SQA 3 by the metallic container of trapezoid conic, 410 mm in upper diameter, 300 mm in lower diameter, and 420mm in height after the execution work for each concrete.

Physical and mechanical properties

The physical properties of the fresh concrete are exceeded over the design properties as indicated in Table 5. The 1/10-low-activation concrete, however, requires less bleeding rate in the case of applying to a nuclear facility. The data of the compressive strength for the 1/10- and 1/30-low-activation concrete are also considered to be excellent as presented in Fig. 1. Figure 2 shows the relationship between the compressive strength and splitting tensile strength based on experiment result. In general, development of the splitting tensile strength with respect to concrete age can be estimated by the compressive strength. Examples are shown in Eq. (1) and Eq. (2) proposed by Japan society of Civil Engineers [5].

Table 1. Dominant target element of reference material [4]

No.	Material	Place	Co(ppb)	Eu(ppb)
1	Andesite (Geostandard sample, JA-1)	Japan	12,300	1,200
2	Limestone aggregate A	Fukushima, Japan	20	20
3	Limestone aggregate B	Okayama, Japan	70	52
4	Limestone aggregate C	Fukushima, Japan	8.4	9.3
5	Limestone aggregate D	Aomori, Japan	41	7.0
6	Limestone aggregate E	Saitama, Japan	44	15.7
7	Ordinary Portland cement A	Japan	9,000	690
8	Low heat Portland cement A	Japan	10,000	290
9	White cement A	Japan	1,590	280

Table 2. Mix proportion

Type of low-activation concrete	W/C (%)	s/a (%)	Composition (kg/m^3)			
			Water	Cement	Fine aggregate	Coarse aggregate
1/10-low-activation concrete (Limestone aggregate + Low heat Portland cement)	50	49	175	350	899	913
1/30-low-activation concrete (Limestone aggregate + White cement)	50	46	158	316	855	1,018

Table 3. Density and water absorption rate

Material		Density (g/cm^3)	Water absorption rate (%)
Cement	Low heat Portland cement	3.13	—
	White cement	3.05	—
Fine aggregate	Limestone (Aomori, Japan)	2.67	0.99
Coarse aggregate		2.70	0.21

Table 4. Test and inspection

Item	Criteria	Remarks
Slump	JIS A 1101	-
Air content	JIS A 1128	-
Concrete temperature	-	Used thermometer
Setting time	JIS A 1147	Automatic machine
Bleeding water	JIS A 1123	-
Compressive strength	JIS A 1108	Standard curing
Splitting tensile strength	JIS A 1113	Sealed curing
Young's modulus	JIS A 1149	Compressive meter
Setting time	JIS A 1147	Automatic machine
Adiabatic temperature rise	JCI SQA3	Air circulation type

$$f'_c(t) = \frac{t}{a + bt} \cdot f'_c(28) \cdot d \quad (1)$$

$$f_{tk}(t) = c\sqrt{f'_c(t)} \quad (2)$$

where,

$f'_c(t)$: compressive strength of concrete at an age of t days, in N/mm^2,
$f_{tk}(t)$: splitting tensile strength of concrete at an age of t days, in N/mm^2,
$f'_c(28)$: compressive strength of concrete at an age of 28 days, in N/mm^2,
t : age, in day,
a,b : coefficient concerning increasing ratio of compressive strength, though they vary with type of cement.
c : taken as 0.44 in standard practice, though it values with such factors as degree of drying of concrete.
d : increasing ratio of compressive strength of 91 days against that of 28 days.

The compressive strength at an age of 28 days and coefficients a, b and d calculated from the experiment result are shown in Fig. 1. The splitting tensile strength obtained from experiment is distributed larger than splitting tensile strength estimated by Eq (2). The approximation curve calculated from the experiment result is separately shown in Fig. 2.

Figure 3 shows the relationship between the compressive strength and young's modulus based on the experiment result. As a method for early dealing with stiffness change due to hydration and stress relaxation due to creep, the method of calculating thermal stress by effective Young's modulus was proposed. When a simplified method to estimate the effective Young's modulus is needed, Eq. (3) can be used [5]. The line of Eq. (3) is drawn in Fig. 3. It can be seen from Fig. 3 that the experimental results and Eq. (3) are in close agreement.

Table 5. Physical properties of fresh concrete

Material	Slump (cm)	Air content (%)	Concrete temperature (ºC)	Density (kg/m^3)	Percentage of bleeding capacity (%)	Setting time	
						Initial (hr-min)	Final (hr-min)
1/10-low-activation concrete	12.5	4.6	20.7	2,340	11.4	7-08	4-31
1/30-low-activation concrete	13.5	3.1	21.1	2,384	2.3	9-46	6-11

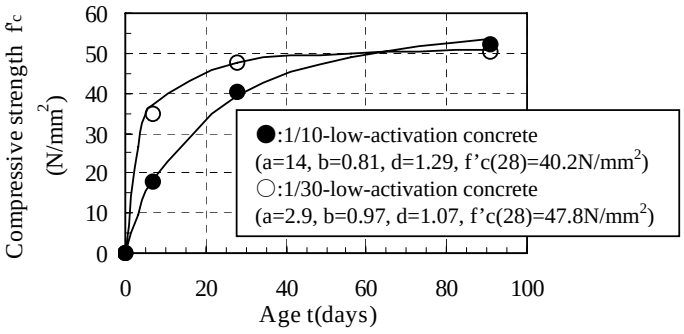

Fig. 1 Relationship between age and compressive strength

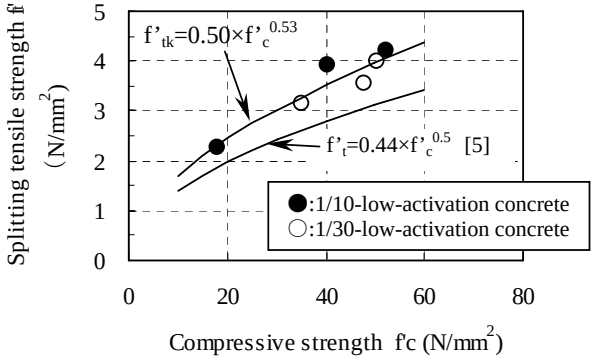

Fig. 2 Relationship between compressive strength and splitting tensile strength

$$E_c(t) = \phi(t) \cdot 4.7 \times 10^3 \cdot \sqrt{f'_c(t)} \quad (3)$$

where,

$E_c(t)$: effective Young's modulus at the age of t days, in N/mm^2,

ϕ (t) : compensating factor taking account of creep during concrete temperature increasing

for up to 3 days : ϕ =0.73

for up to 5 days : ϕ =1.00

from 3 days to 5 days: linear interpolation can be used.

$f'_c(t)$: compressive strength of concrete at an age of t days, in N/mm^2.

Adiabatic temperature rise

The adiabatic temperature rises of the 1/10- and 1/30-low-activation concrete are shown in Fig. 4, with the adiabatic temperature rise of the ordinary concrete proposed by Japan Society of Civil Engineers [5]. The adiabatic temperature rise, Q (t), is derived from estimated the ultimate temperature rise and the coefficient concerning temperature rise speed by the experiment of the adiabatic temperature rise.

$$Q(t) = Q_{max} \ [1-\exp(-\alpha \times t^{\beta})] \quad (4)$$

where,

Q(t): adiabatic temperature rise, in ºC,

Q_{max}: ultimate temperature rise, in ºC,

t: age, in day,

α, β : coefficient concerning temperature rise speed.

The ultimate temperature rise, coefficient α, and β calculated from the experiment result are shown in Fig. 4. The values of the ultimate temperature rise for the 1/10- and 1/30-low-activation concrete are small compared to that of the ordinary concrete. As the 1/10-low-activation concrete is composed of the low-heated Portland cement, the coefficient α of the 1/10-low-activation concrete is very small.

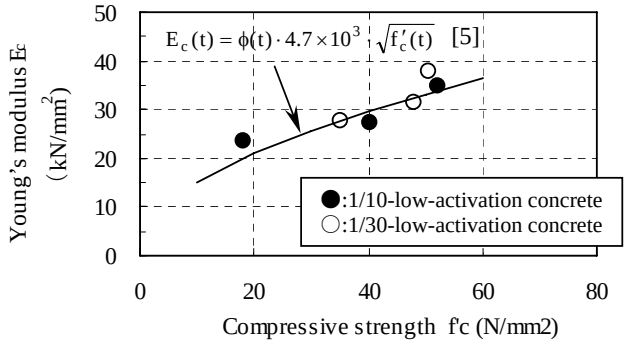

Fig. 3 Relationship between compressive strength and young's modulus

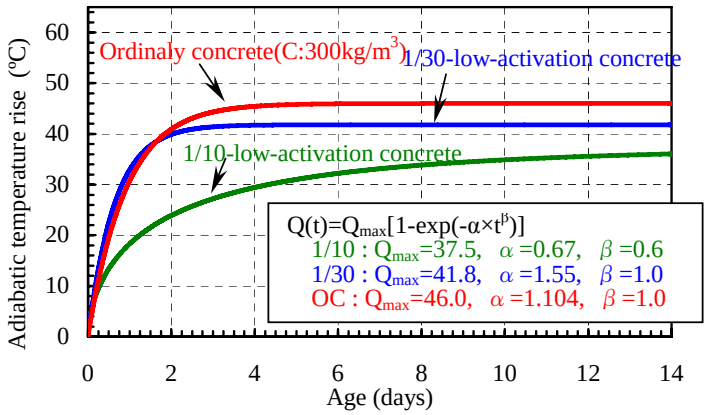

Fig. 4 Adiabatic temperature rise

THERMAL STRESS ANALYSES

Analytical condition

The thermal stress analyses were carried out under the assumption of the application for shielding wall. The thermal stress analyses were executed by a three-dimension finite element method, with the cylindrical model of 45 degrees cited by Architectural Institute of Japan [6], by Q(t) from the results of the adiabatic temperature rise shown in Fig. 4 and by mechanical properties shown in Fig. 1, Fig. 2 and Fig. 3. The analytical model of the concrete wall and the boundary condition of the heat transfer are shown in Fig. 5. The initial temperature of the concrete, the outside atmospheric temperature and the ground initial temperature were assumed to be 20 ºC. The placing of concrete was assumed to be divided into three portions, i.e. the base concrete, the 1st lift of the reactor shielding wall, and the 2nd lift of portions in the order of the execution works. The placing of the 1st lift concrete of the wall was executed after the base concrete execution for 28 days later. The placing of the 2nd lift concrete was also executed another 28 days later after the execution of 1st lift concrete. The executed concrete was assumed to be faced to the form for first seven days and be faced to the atmosphere after 7 days curing. The analysis was executed for 147 days, from the time of the placing of base concrete to the 91 days after the placing of end of the 2nd lift concrete. Thermo data used in thermal stress analysis is shown in Table 6. The coefficient of thermal expansion of the concrete is 0.00001/ºC. The crack resistances of the massive concrete for the node red circle sign, which located at the surface and center of the section A and B in Fig. 5, were evaluated.

Cracking index

Japan Society of Civil Engineers (JSCE) proposed the thermal "cracking index" as the index for the appearance of the thermal cracking in the concrete[5]. The cracking index is defined as the ratio of the splitting tensile strength of the concrete to the tensile stress in the concrete generated by heat of hydration defined Eq. (5), as follows,

$$i_c(t)=f_{tk}(t)/\sigma_t(t) \tag{5}$$

where,
$i_c(t)$:cracking index at age of t days,
$f_{tk}(t)$:splitting tensile strength of concrete at age of t days, which is defined by Eq. (2)
$\sigma_t(t)$:tensile stress in concrete at age of t days, which is defined the multiplication of the strain obtained by FEM analysis and the effective Young's modulus at the age of t days by Eq. (3)

Analytical result

The results of the thermal stress analyses are summarized in Table 7. The table presents that the maximum temperature rise of the concrete and the minimum cracking index of section A and B. The thermal cracking index has

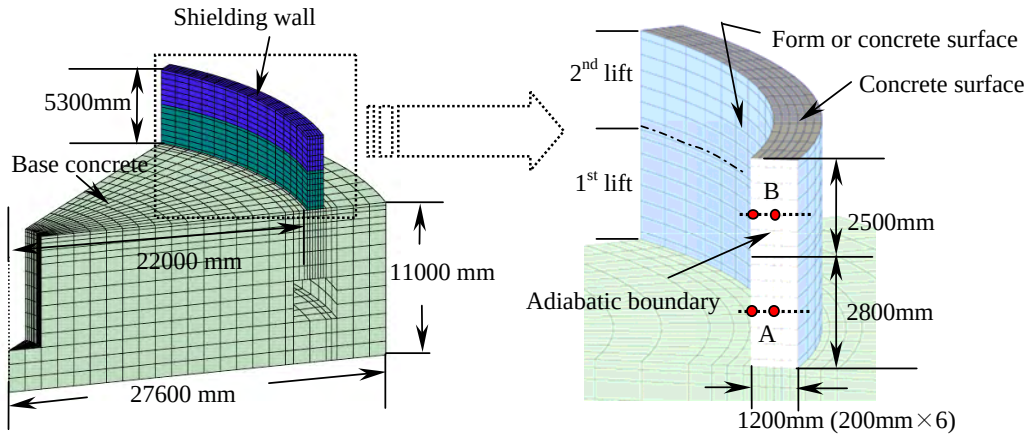

a) Analytical model [6] b) Boundary condition of heat transfer

Fig. 5 Analytical model of shielding wall and boundary condition

Table 6. Thermo data used in thermal stress analysis

Material	Specific heat (kJ/kg·ºC)	Thermal conductivity (Wm·ºC)	Density (kg/m^3)	Heat transfer coefficient (W/m^2·ºC)	
				Form	Concrete surface
Concrete	1.15	2.7	2,350	8.0	12.0
Ground	0.800	1.7	2,600	—	—

Table 7. Maximum temperature and minimum cracking index (1200 mm in thickness)

Material	1st lift (Section A)				2nd lift (Section B)			
	Maximum concrete temperature rise CT		Minimum cracking index ic		Maximum concrete temperature rise CT		Minimum cracking index ic	
	CT (ºC)	Age(days)	ic	Age(days)	CT (ºC)	Age(days)	ic	Age(days)
1/10-low-activation concrete	18.6	1.8	1.47	1.0	18.5	1.6	1.52	1.0
1/30-low-activation concrete	32.8	1.4	0.93	1.0	32.8	1.4	1.00	1.1

been conventionally used in the verification of cracking due to volume changes caused by heat generation by the hydration of cement for massive concrete. The larger cracking index, the generation possibility of crack occurrence is lesser, while, the number of cracks increases and the crack width tends to grow larger, upon smaller cracking index. The value of the minimum cracking index to prevent the crack generation is recommended to be 1.45-1.75 by JSCE [5]. The probability of the crack generation is estimated to be 5% for the cracking index of 1.75, to be 25% for the cracking index of 1.45, and also to be 85% for the cracking index of 1.0. The minimum cracking index of the 1/10-low-activation concrete is 1.47, and that for the 1/30-low-activation concrete is 0.93. These results conduct the proper utilization of the 1/10-low-activation concrete for applying massive concrete in the reactor, and further improvement of the 1/30-low-activation concrete regarding on the property of the massive concrete.

For the above improvement of the 1/30-low-activation concrete, another analysis was executed by the Q_{max} value for 1/10-low-activation concrete with α=1.00 and β=1.0 in the same mechanical properties. The craking index was calculated 1.5, which could be target of the heat reduaction of the 1/30-low-activation concrete. However, it is known that the strength decreases with decreasing heat of hydration. So, in order to improve ultimate temperature rise Q_{max} and coefficient concerning temperature rise speed α of the 1/30-low-activation concrete, another work has been performed for the low activation concrete with the low-activation admixture obtained by the screening test [7].

CONCLUSIONS

The results of this study are summarized as follows,

1) The realization of the two types of low-activation concrete－the 1/10-low-activation concrete composed of the low-heated Portland cement and high-purity limestone aggregates, and the 1/30-low-activation concrete composed of the white cement and high-purity limestone aggregates－ are evaluated by the experimental works.
2) The preliminary FEM analysis of thermal stress for the low-activation concrete conducts that the 1/10-low-activation concrete can be utilized for a structure member of the shielding wall.
3) The 1/30-low-activation concrete is also applicable to that by the above analysis in certain condition, but requires further improvement on the high-heat problems to apply to massive concrete in the reactors.

ACKNOWLEDGMENT

We express our grateful appreciation to Dr. M. Uematsu of Toshiba Co., Dr. K. Hayashi of Hitachi Ltd., Mr. M. Nakata of Mitsubishi Heavy Industries, Ltd., Mr. M. Saito of Tohoku Electric Power Co., Inc., Dr. T. Tanosaki of Taiheiyo Cement Co., Mr. R. Yoshino of Denki Kagaku Kogyo K.K. and Mr. M. Sato of Nippon Steel Techno research Co. for discussions and comments. This work is supported by a grant-in-aid of Innovative and Viable Nuclear Technology (IVNET) development project of Ministry of Economy, Trade and Industry, Japan.

REFERENCE

1. Kinno, M., “The Present Activities on Low-activation.” Japan Concrete Institute, *Concrete Journal,* Vol.42, No.6, 2004, pp.3-10.
2. IAEA, “Application of the concepts of exclusion, exemption and clearance”, Safety standards series No. RS-G-1.7, International Atomic Energy Agency, 2004.
3. Kinno, M. et al., “Raw Materials for Low-Activation Concrete Neutron Shield”, Journal of Nuclear Science and Technology, Vol.39, No.12, 2002, pp.1275-1280.
4. Hasegawa, A. et al., “Development of Low-Activation Design Method for Reduction of Radioactive Waste below Clearance Level”, Innovative and Viable Nuclear Energy Technology (IVNET) Development Project, Ministry of Economy, Trade and Industry, Japan, 2006.
5. JSCE, “STANDARD SPECIFICATION FOR CONCRETE STRUCTURES-2002, Materials and Construction.”, Japan Society of Civil Engineers, 2002.
6. AIJ, “State of The Art Report on Mass Concrete,” Architectural Institute of Japan, 2001.
7. Kimura, K. et al., “Development of Low-Activation Design Method for Reduction of Radioactive Waste below Clearance Level (12) –Low-Activation Admixture–.” 2006 Annual Mtg., Atomic Energy Society of Japan.